Grid integration of distributed renewable energy: Volt/Var control with high penetration of solar PV generations

- ***Coordination*** between voltage regulation devices and PV smart inverters
- Real-time volt/var control
- IEEE 1547-2018 Standard

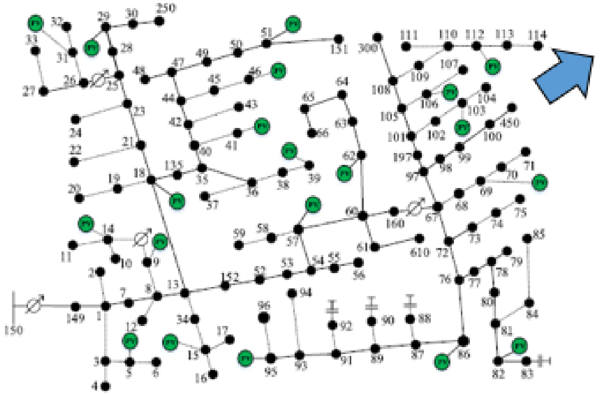

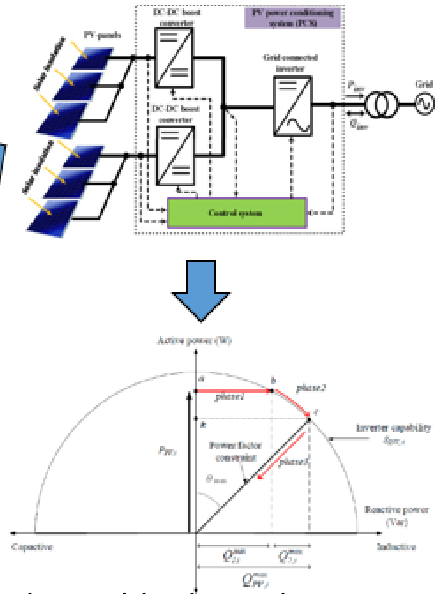

- Conservation voltage reduction

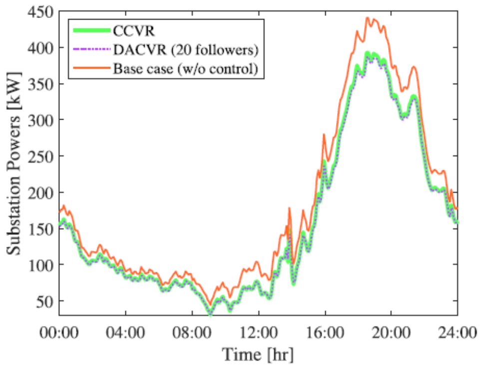

- Regulate grid-edge voltage

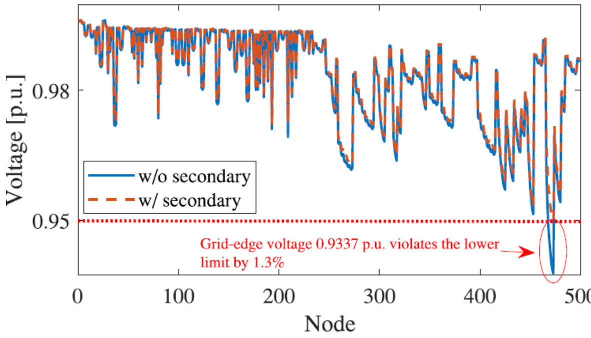

- ***ADMM-based distributed control*** method: decompose large-scale problem, exchange information, privacy
  - Bus-level distributed control
  - Network-level distributed control

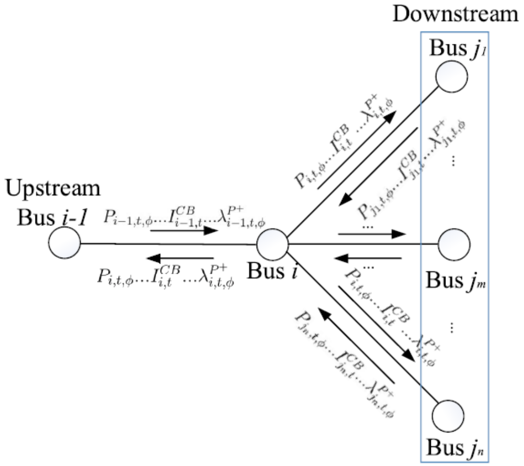

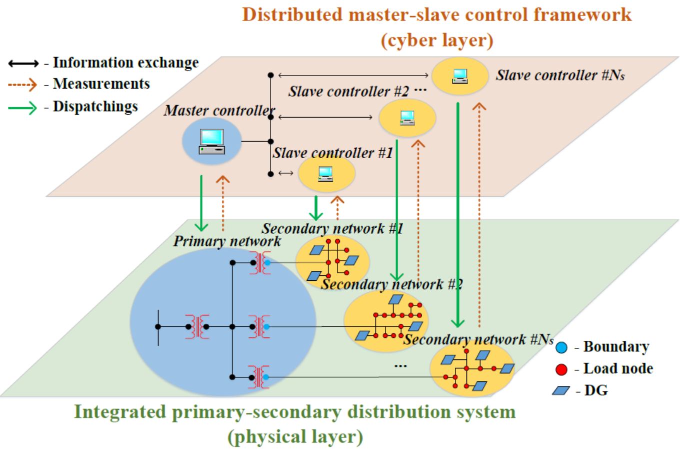

- Q. Zhang, K. Dehghanpour and Z. Wang, "Distributed CVR in Unbalanced Distribution Systems With PV Penetration," in IEEE Transactions on Smart Grid, vol. 10, no. 5, pp. 5308-5319, Sept. 2019.
- Q. Zhang, Y. Guo, Z. Wang and F. Bu, "Distributed optimal conservation voltage reduction in integrated primary-secondary distribution systems," IEEE Trans. Smart Grid, vol. 12, no. 5, pp. 3889-3900, Sept. 2021.

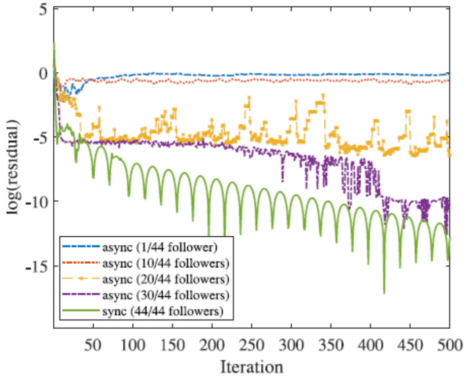

- Online and asynchronous implementations
- Robust against non-uniform update rates and communication delays
- Make our application more suitable for real-world applications

Main contributions of distributed CVR in distribution system

Distribution systems:

- Unbalanced three-phase distribution systems
- Integrated primary-secondary distribution networks
- Online feedback measurement-based linear approximation method
- Coordination between voltage regulation devices and smart inverters

Distributed optimization methods:

- Propose a projection ADMM-based method to handle the non-convex optimization problem with discrete switching and tap changing variables
- Propose an asynchronous ADMM-based method, which is robust against non-uniform update rates and communication delays

Outline

- **Distributed Optimal Conservation Voltage Reduction in Integrated Primary-Secondary Distribution Systems**
  - **Integrated primary-secondary distribution networks**
  - **Distributed leader-follower optimization, online and asynchronous implementations**
  - **Results**

Introduction: Volt/Var Control

- Conventional voltage regulation devices
- Slow timescale (hourly)

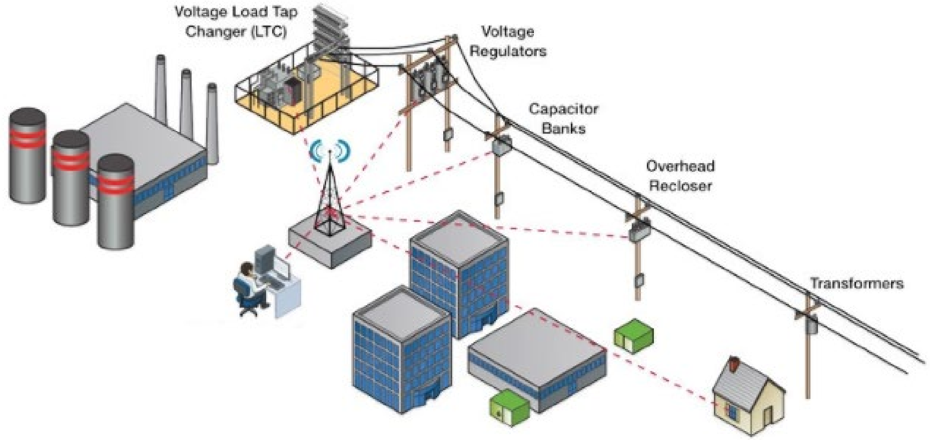

Load tap changer

Voltage regulator

Capacitor bank

- Increasing integration of distributed energy resources (DERs), e.g., residential solar photovoltaics (PVs)
- Fast timescale (seconds/minutes)

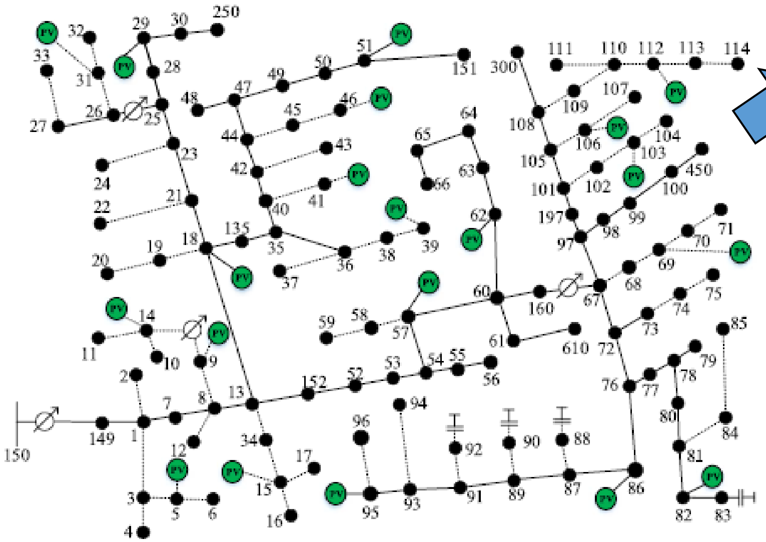

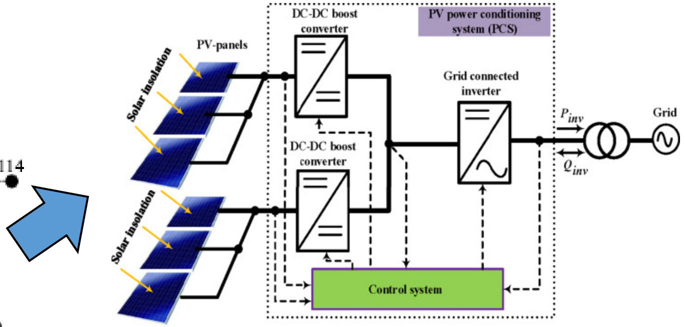

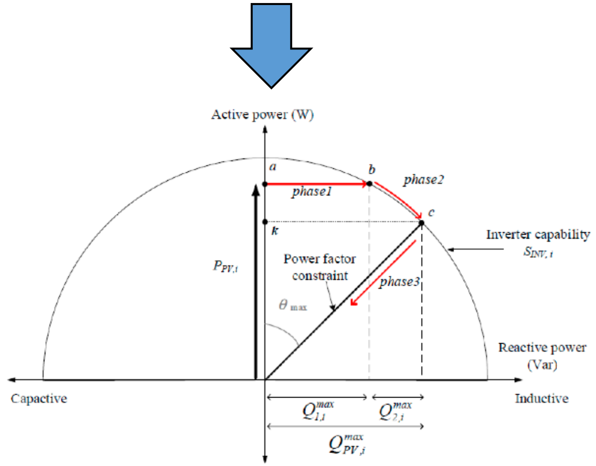

- Office of Electricity Delivery and Energy Reliability, "Voltage and VAR Control Impact Analysis Approach", U.S. Department of Energy
- Hsieh, S.-C.; Lee, Y.-D.; Chang, Y.-R. Economic Evaluation of Smart PV Inverters with a Three-Operation-Phase Watt-Var Control Scheme for Enhancing PV Penetration in Distribution Systems in Taiwan. *Appl. Sci.* **2018**, *8*, 995.
- A. Motin, S. Sadoyama, L. R. Roose, and S. Sepasi, "Distributed Voltage Regulation using VVC of a Smart PV Inverter in a Smart Grid"

Introduction: Conservation Voltage Reduction

What is CVR ?

<u>Conservation voltage reduction (CVR)</u> lowers distribution voltage levels to reduce energy consumption and peak demand.

- Short-term (peak-time) CVR
- Long-term (24-hr) CVR

90% of homes receive voltage at the high-end of ANSI range

Nature of CVR

- Load is sensitive to voltage

Why is CVR?

Power consumption reduction by reducing supplied volt from 122 V to 116 V

Appliance	Conserved Power (W)	Conserved Power (%)
Induction Motor		
Fan	4.2	6%
Display		
CRT TV	2.1	4%
LCD TV	0	0
Plasma TV	-2	0
Lighting		
13- W Compact Fluorescent Lamp (CFL)	0.9	8%
20- W CFL	1	6%
42-W CFL	0.8	2%
LED	0.2	6%
75- W Incandescent	3.4	5%

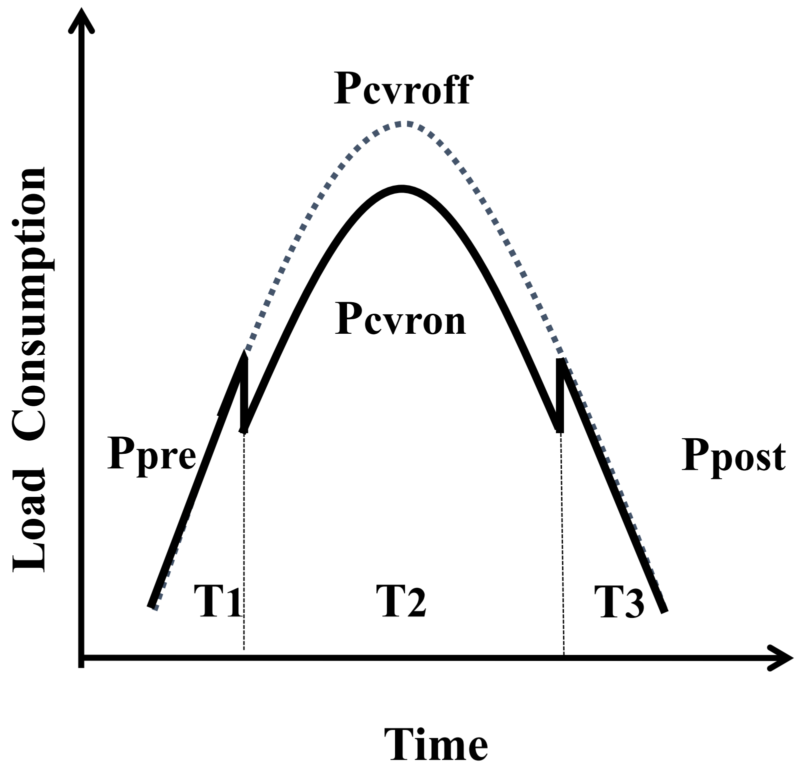

K. Warner, and R. Willoughby, National Assessment of CVR-Preliminary Results from DOE's CVR Initiative, IEEE Smart Grid Webinar, Sep. 11, 2014.

Integrated Primary-Secondary Distribution Networks

A practical distribution system: medium-voltage (MV) primary networks + low-voltage (LV) secondary networks.

- Most loads and residential DERs are connected to secondary networks.
- The secondary networks are simplified by using aggregate models.
- The grid-edge voltage regulation is not well addressed with aggregate models.

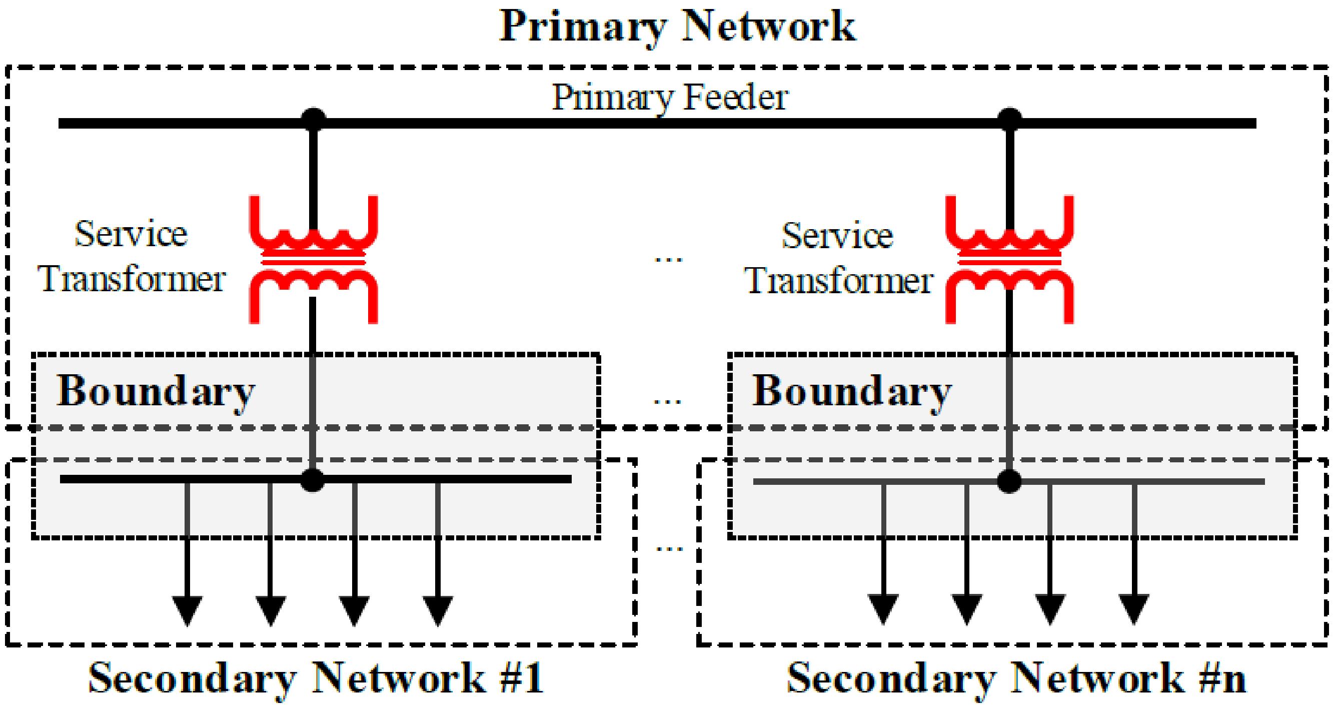

- The coupling constraints at boundary nodes between primary network and secondary network

$$p_{i,\phi,t} + \sum_{j \in \mathcal{N}_i} P_{i'j,\phi,t} = 0, \forall i \in \mathcal{B}$$

$$q_{i,\phi,t} + \sum_{j \in \mathcal{N}_i} Q_{i'j,\phi,t} = 0, \forall i \in \mathcal{B}$$

$$v_{i,\phi,t} - v_{i',\phi,t} = 0, \forall i \in \mathcal{B}$$

Nonlinear Terms in Power Flow Models

Unbalanced three-phase distribution systems

- DistFlow model has nonlinear term
- Linearized distribution power flow (Lin-DistFlow) model neglected the nonlinear terms

$$\sum_{k\in\Omega_k(i\cdot)} P^K_{k,\phi_a} - \sum_{k\in\Omega_k(\cdot,i)} P^K_{k,\phi_a} = P^G_{i,\phi_a} - P^L_{i,\phi_a} + \varepsilon^p_{i,\phi_a}$$

$$\sum_{k\in\Omega_k(i\cdot)} Q^K_{k,\phi_a} - \sum_{k\in\Omega_k(\cdot,i)} Q^K_{k,\phi_a} = Q^G_{i,\phi_a} - Q^L_{i,\phi_a} + \varepsilon^q_{i,\phi_a}$$

$$\sum_{k\in\Omega_k(i\cdot)} P^K_{k,\phi_b} - \sum_{k\in\Omega_k(\cdot,i)} P^K_{k,\phi_b} = P^G_{i,\phi_b} - P^L_{i,\phi_b} + \varepsilon^p_{i,\phi_b}$$

$$\sum_{k\in\Omega_k(i\cdot)} Q^K_{k,\phi_b} - \sum_{k\in\Omega_k(\cdot,i)} Q^K_{k,\phi_b} = Q^G_{i,\phi_b} - Q^L_{i,\phi_b} + \varepsilon^q_{i,\phi_b}$$

$$\sum_{k\in\Omega_k(i\cdot)} P^K_{k,\phi_c} - \sum_{k\in\Omega_k(\cdot,i)} P^K_{k,\phi_c} = P^G_{i,\phi_c} - P^L_{i,\phi_c} + \varepsilon^p_{i,\phi_c}$$

$$\sum_{k\in\Omega_k(i\cdot)} Q^K_{k,\phi_c} - \sum_{k\in\Omega_k(\cdot,i)} Q^K_{k,\phi_c} = Q^G_{i,\phi_c} - Q^L_{i,\phi_c} + \varepsilon^q_{i,\phi_c}$$

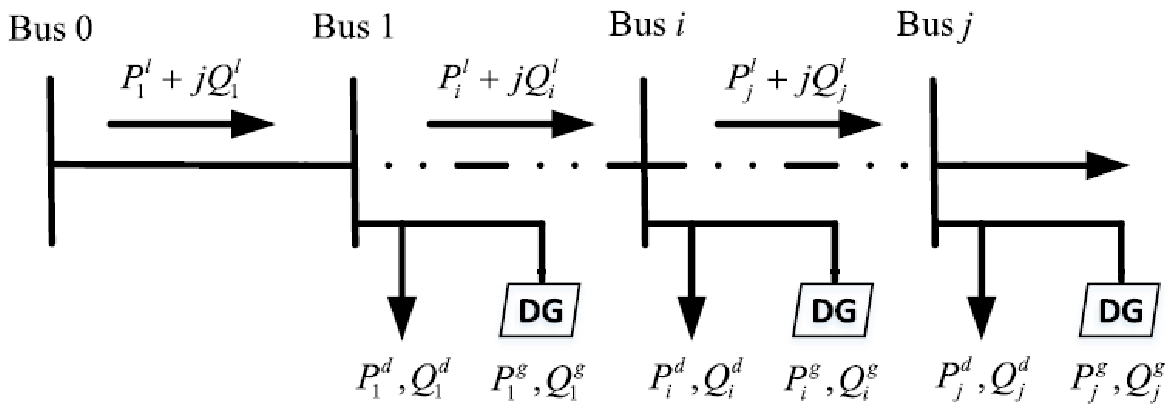

$$v_{i,\phi_a} - v_{j,\phi_a} = 2\left(\hat{R}_{aa}P^K_{k,\phi_a} + \hat{R}_{ab}P^K_{k,\phi_b} + \hat{R}_{ac}P^K_{k,\phi_c} + \hat{X}_{aa}Q^K_{k,\phi_a} + \hat{X}_{ab}Q^K_{k,\phi_b} + \hat{X}_{ac}Q^K_{k,\phi_c}\right) + \varepsilon^v_{ij,\phi_a}$$

$$v_{i,\phi_b} - v_{j,\phi_c} = 2\left(\hat{R}_{ba}P^K_{k,\phi_a} + \hat{R}_{bb}P^K_{k,\phi_b} + \hat{R}_{bc}P^K_{k,\phi_c} + \hat{X}_{ba}Q^K_{k,\phi_a} + \hat{X}_{bb}Q^K_{k,\phi_b} + \hat{X}_{bc}Q^K_{k,\phi_c}\right) + \varepsilon^v_{ij,\phi_b}$$

$$v_{i,\phi_c} - v_{j,\phi_c} = 2\left(\hat{R}_{ca}P^K_{k,\phi_a} + \hat{R}_{cb}P^K_{k,\phi_b} + \hat{R}_{cc}P^K_{k,\phi_c} + \hat{X}_{ca}Q^K_{k,\phi_a} + \hat{X}_{cb}Q^K_{k,\phi_b} + \hat{X}_{cc}Q^K_{k,\phi_c}\right) + \varepsilon^v_{ij,\phi_c}$$

Voltage-dependent loads:

- ZIP load has nonlinear term

Bus Type	Zp	Ip	Pp	Zq	Iq	Pq
Commercial	0.43	-0.06	0.63	4.06	-6.65	4.49
Residential	0.85	-1.12	1.27	10.96	-18.73	8.77
Industrial	0	0	1	0	0	1

$$\hat{Z}_k = a_\phi a_\phi^H \odot Z_k = \begin{bmatrix} Z_{aa} & Z_{ab}e^{-\frac{j2\pi}{3}} & Z_{ac}e^{\frac{j2\pi}{3}} \\ Z_{ba}e^{\frac{j2\pi}{3}} & Z_{bb} & Z_{bc}e^{\frac{-j2\pi}{3}} \\ Z_{ca}e^{\frac{-j2\pi}{3}} & Z_{cb}e^{\frac{j2\pi}{3}} & Z_{cc} \end{bmatrix} \qquad a_\phi = \left[1, e^{-2\pi/3}, e^{2\pi/3}\right]^T$$

$$\hat{R}_k = real\left(\hat{Z}_k\right) = \begin{bmatrix} \hat{R}_{aa} & \hat{R}_{ab} & \hat{R}_{ac} \\ \hat{R}_{ba} & \hat{R}_{bb} & \hat{R}_{bc} \\ \hat{R}_{ca} & \hat{R}_{cb} & \hat{R}_{cc} \end{bmatrix} \qquad \hat{X}_k = imag\left(\hat{Z}_k\right) = \begin{bmatrix} \hat{X}_{aa} & \hat{X}_{ab} & \hat{X}_{ac} \\ \hat{X}_{ba} & \hat{X}_{bb} & \hat{X}_{bc} \\ \hat{X}_{ca} & \hat{X}_{cb} & \hat{X}_{cc} \end{bmatrix}$$

Q. Zhang, K. Dehghanpour and Z. Wang, "Distributed CVR in Unbalanced Distribution Systems With PV Penetration," in IEEE Transactions on Smart Grid, vol. 10, no. 5, pp. 5308-5319, Sept. 2019

Distributed Optimal CVR in Integrated Primary-Secondary Distribution Systems

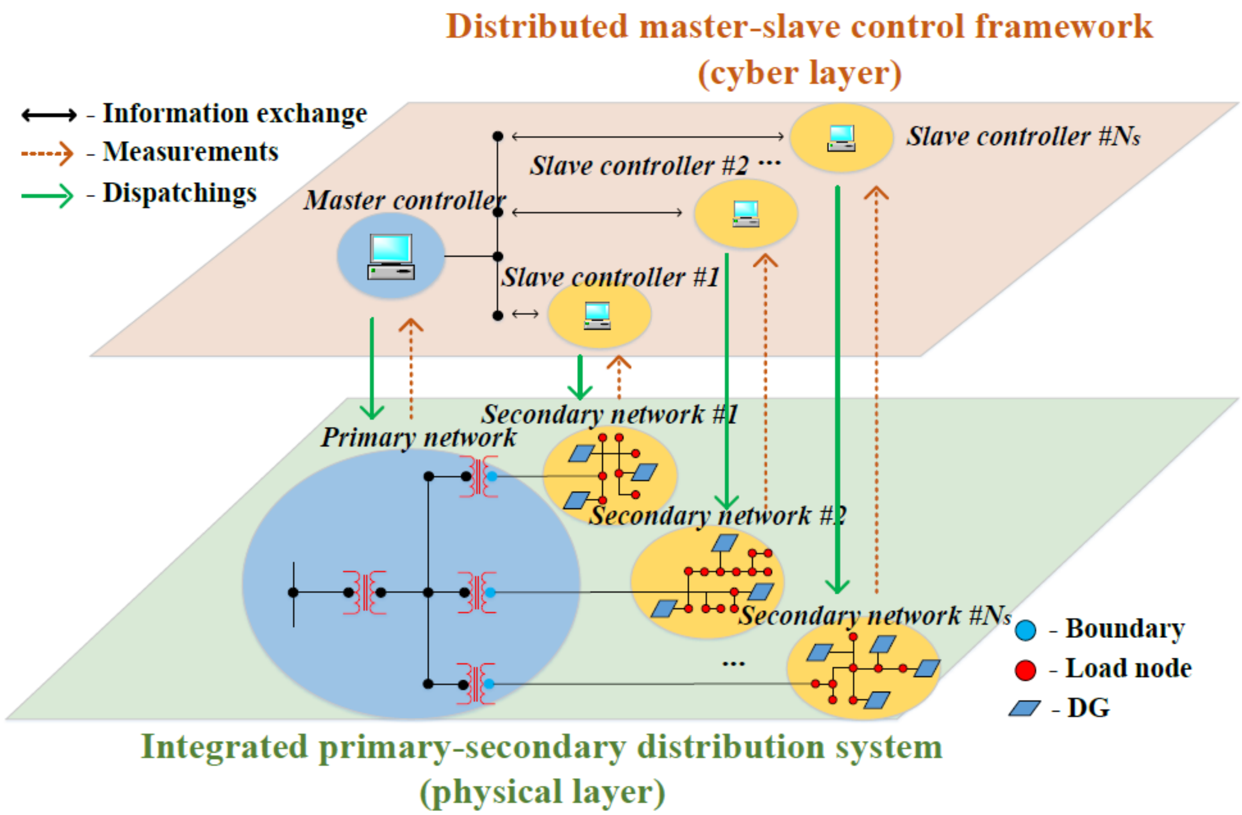

- Q. Zhang, Y. Guo, Z. Wang and F. Bu, "Distributed Optimal Conservation Voltage Reduction in Integrated Primary-Secondary Distribution Systems," in IEEE Transactions on Smart Grid, vol. 12, no. 5, pp. 3889-3900, Sept. 2021

- Funded by DOE project "Optimal Operation and Impact Assessment of Distributed Wind For Improving and Resilience of Rural Electricity System".
- Funded by NSF project "Data-driven Voltage Var Optimization Enabling Extreme Integration of Distributed Solar Energy"

Mapping Primary-Secondary Distribution System to ADMM-Based Leader-Follower Control Framework:

- Exchange aggregate information at boundaries
- Better model the impacts of DERs
- Improve the grid-edge voltage regulation performance

Online Feedback-Based Linear Approximation Method for Power Flow and ZIP Load:

- The instantaneous power and voltage measurements
- Reduce the computational complexity and linearization errors

Asynchronous implementation

- Robust against non-uniform update rates and communication delays
- Make our application more suitable for real-world applications

Volt/Var Optimization-based CVR

Objective: Minimize the total power consumption of the entire system

$$\min \sum_{j:0\rightarrow j} \sum_{\phi\in\{a,b,c\}} Re\{S_{0j,\phi,t}\}$$

- $Re\{S_{0j,\phi,t}\}$ denotes the three-phase active power supplied from the substation on the feeders.

Constraints: Satisfy a feasible voltage profile across the integrated primary-secondary distribution system and other operational constraints

- Active and reactive power balance on each node:

$$P_{ij,\phi,t} = \sum_{k:j\rightarrow k} P_{jk,\phi,t} - p^{g}_{j,\phi,t} + p^{ZIP}_{j,\phi,t} + \varepsilon^{p}_{ij,\phi,t}$$

$$Q_{ij,\phi,t} = \sum_{k:j\rightarrow k} Q_{jk,\phi,t} - q^{g}_{j,\phi,t} + q^{ZIP}_{j,\phi,t} + \varepsilon^{q}_{ij,\phi,t}$$

- ***$\varepsilon^{p}_{ij,\phi,t}$ and $\varepsilon^{q}_{ij,\phi,t}$ denote the nonlinear terms.***

- Active and reactive ZIP loads:

$$p^{ZIP}_{i,\phi,t} = p^{ZIP,0}_{i,\phi,t} \odot \left(k^{p}_{i,1} v_{i,\phi,t} + k^{p}_{i,2}\sqrt{v_{i,\phi,t}} + k^{p}_{i,3}\right)$$

$$q^{ZIP}_{i,\phi,t} = q^{ZIP,0}_{i,\phi,t} \odot \left(k^{q}_{i,1} v_{i,\phi,t} + k^{q}_{i,2}\sqrt{v_{i,\phi,t}} + k^{q}_{i,3}\right)$$

- $k^{p}_{i,1}$, $k^{p}_{i,2}$, $k^{p}_{i,3}$ and $k^{q}_{i,1}$, $k^{q}_{i,2}$, $k^{q}_{i,3}$ are constant-impedance (Z), constant-current (I) and constant-power (P) coefficient.
- ***$\sqrt{v_{i,\phi,t}}$ is nonlinear term.***

Volt/Var Optimization-based CVR

- Voltage drop through lines and nodal voltage upper and lower bounds :

$$v_{j,\phi,t} = v_{i,\phi,t} - 2(\bar{r}_{ij} \odot P_{ij,\phi,t} + \bar{x}_{ij} \odot Q_{ij,\phi,t}) + \varepsilon^{v}_{ij,\phi,t}$$

$$v^{min} \leq v_{i,\phi,t} \leq v^{max}$$

- $v_{i,\phi,t}$ is the vector of three-phase squared voltage magnitude
- ***$\varepsilon^{v}_{ij,\phi,t}$ denotes the nonlinear term***

- ***Reactive power output of smart inverter:***

$$-q^{cap}_{i,\phi,t} \leq q^{g}_{i,\phi,t} \leq q^{cap}_{i,\phi,t}$$

$$q^{cap}_{i,\phi,t} = \sqrt{\left(s^{g}_{i,\phi,t}\right)^2 - \left(p^{g}_{i,\phi,t}\right)^2}$$

- Requitement for reactive power capacity of the DERs in IEEE 1547-2017 Standard

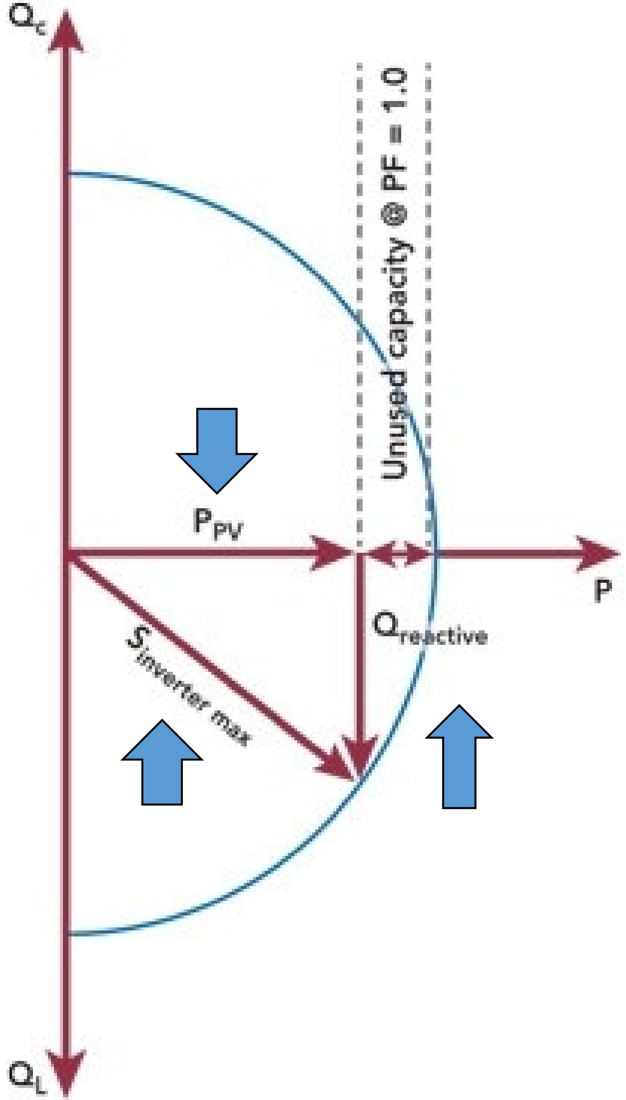

- Compact form of the VVO-based CVR:

$$\min_{x,z_n,\forall n} f(x)$$

s.t. $x \in \chi \coloneqq \{x | constraints\ for\ primary\ network\}$

$$z_n \in \mathcal{Z}_n \coloneqq \{z_n | constraints\ for\ secondary\ networks\}, \forall n$$

$$A_n \odot x_{B,n} + B_n \odot z_{B,n} = 0, \forall n$$

- Decompose the constraints into primary network and secondary networks
- Compact form of the coupling constraints at boundary nodes

T. A. Nguyen, R. Rigo-Mariani, M. A. Ortega-Vazquez and D. S. Kirschen, "Voltage Regulation in Distribution Grid Using PV Smart Inverters," 2018 IEEE Power & Energy Society General Meeting (PESGM), 2018, pp. 1-5.

Standard Distributed Solution via ADMM

- The ***alternating direction method of multipliers (ADMM)*** solves the VVO-based CVR problem by iteratively minimizing the augmented Lagrangian:

Objective funciton

ρ^k is the iterative (k) varying penalty coefficient for constraint violation

$$L_\rho = \underbrace{f(x)}_{\text{Objective funciton}} + \sum_{n=1}^{N_s} \underbrace{\lambda_n \odot \left(A_n \odot x_{B,n} + B_n \odot z_{B,n}\right)} + \sum_{n=1}^{N_s} \overbrace{\frac{\rho^k}{2}\left\|A_n \odot x_{B,n} + B_n \odot z_{B,n}\right\|_2^2}$$

λ_n is the vector of the Lagrange multiplier

- The ***leader controller*** first updates the variable x associated with ***primary system*** and send the updated boundary variables $x_{B,n}^{k+1}$ to follower controller:

$$x^{k+1} = \underset{x\in\mathcal{X}}{\operatorname{argmin}}\, f(x) + \sum_{n=1}^{N_s} \lambda_n^k \odot \left(A_n \odot x_{B,n} + B_n \odot z_{B,n}^k\right) + \sum_{n=1}^{N_s} \frac{\rho^k}{2}\left\|A_n \odot x_{B,n} + B_n \odot z_{B,n}^k\right\|_2^2$$

- The nth ***follower controller*** updates the variable z_n associated with the ***secondary system*** and send the updated boundary $z_{B,n}^{k+1}$ to the leader controller:

$$z_n^{k+1} = \underset{z_n\in\mathcal{Z}_n}{\operatorname{argmin}} \sum_{n=1}^{N_s} \lambda_n^k \odot \left(A_n \odot x_{B,n}^{k+1} + B_n \odot z_{B,n}\right) + \frac{\rho^k}{2}\left\|A_n \odot x_{B,n}^{k+1} + B_n \odot z_{B,n}\right\|_2^2$$

- Each follower controller is also responsible for updating the variable λ_n by received $x_{B,n}^{k+1}$ and $z_{B,n}^{k+1}$. The newly updated λ_n^{k+1} will be sent to the leader controller:

$$\lambda_n^{k+1} = \lambda_n^k + \rho^k\left(A_n \odot x_{B,n}^{k+1} + B_n \odot z_{B,n}^{k+1}\right)$$

Asynchronous implementation of ADMM

Sync-ADMM: the leader controller must wait till all the follower controllers finish updating their variables z_n and receive the latest boundary variables $z_{B,n}$, then proceed.

Async-ADMM: the leader controller only needs to receive the updates from several $1 \leq \tilde{N}_S \leq N_S$ follower controllers.

- Partial barrier: A small number of $\tilde{N}_S$ means that the update frequencies of the slow follower controller can be less than those fast follower controller.
- Bounded delay: The *n*th follower controller must communicate with the leader controller for updating local variables at least once every $\tau_n \geq 1$ iterations.

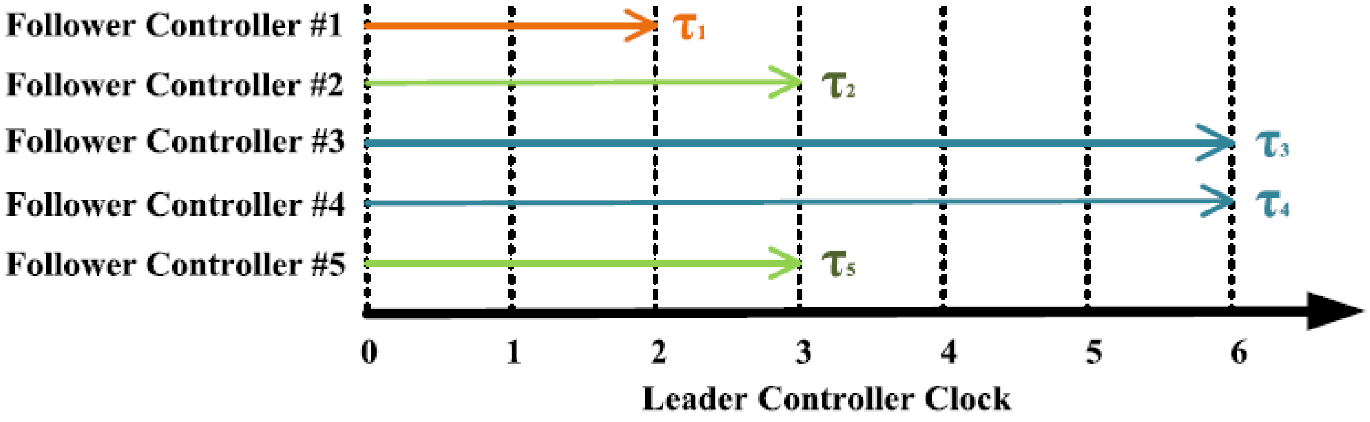

- Partial barrier, $\tilde{N}_S$=2.
- Bounded delay: $\tau_1 = 2, \tau_2 = \tau_5 = 3, \tau_3 = \tau_4 = 6$.
- The leader controller has already preserved the update of follower controller 1 for five iterations and follower controllers 2 and 5 for four iterations.

Asynchronous implementation of ADMM

The ***convergence rate*** of this Async-ADMM is in the order of $O\left(N_s\tau_s/2T\widetilde{N}_S\right)$. T is the total time length for termination.

- Larger N_s leads to larger k. It is because each follower controller's update is less informative with a smaller data subset in each iteration.
- Larger $\widetilde{N}_S$ leads to smaller k. It is because the primary network can collect more information from the secondary networks in each iteration.
- Larger τ_s leads to larger k, due to the very infrequent information exchange between the primary network and the secondary networks.

To further improve the convergence performance and capture fast variations of the Async-ADMM, we implement an iterative varying penalty factor:

$$\rho^{k+1} := \begin{cases} \tau^{inc}\rho^k, if\ \|r^k\|_2 > \mu\|s^k\|_2 \\ \rho^k/\tau^{dec}, if\ \|r^k\|_2 < \mu\|s^k\|_2 \\ \rho^k, otherwise \end{cases}$$

- Primal residual, $r_n^k = A_n \odot x_{B,n}^k + B_n \odot z_{B,n}^k\ , \forall n$
- Dual residual, $s_n^k = \rho^k A_n^T \odot B_n\left(z_{B,n}^{k+1} - z_{B,n}^k\right), \forall n$

$\tau^{inc} > 1$ $\quad \tau^{dec} > 1$ $\quad \mu > 1$

Online Feedback-based Linear Approximation

The ***instantaneous power and voltage measurements*** at time $t-1$ are used as the system feedback to estimate the nonlinear terms $\varepsilon^{p}_{ij,\phi,t}$, $\varepsilon^{q}_{ij,\phi,t}$ and $\varepsilon^{v}_{ij,\phi,t}$:

$$\varepsilon^{p}_{ij,\phi,t} = Re\{(S^{m}_{ij,\phi,t-1} \oslash v^{m}_{i,\phi,t-1}) \odot (v^{m}_{i,\phi,t-1} - v^{m}_{j,\phi,t-1})\}$$

$$\varepsilon^{q}_{ij,\phi,t} = Im\{(S^{m}_{ij,\phi,t-1} \oslash v^{m}_{i,\phi,t-1}) \odot (v^{m}_{i,\phi,t-1} - v^{m}_{j,\phi,t-1})\}$$

$$\varepsilon^{v}_{i,\phi,t} = \left[z_{ij}\left((S^{m}_{ij,\phi,t-1})^{*} \oslash (v^{m}_{i,\phi,t-1})^{*}\right)\right] \odot \left[z^{*}_{ij}(S^{m}_{ij,\phi,t-1} \oslash v^{m}_{i,\phi,t-1})\right]$$

- We assume a widespread coverage of meters throughout the network.
- $S^{m}_{ij,\phi,t-1}$ and $v^{m}_{i,\phi,t-1}$ are instantaneous power and voltage measurements at time *t-1*.
- If we have a small *t*, then the difference of measurements is small between *t-1* and *t*.
- Accurately track the fast variations of renewable generation and load demand for better CVR performance

To handle the non-convexity due to the nonlinear term $\sqrt{v_{i,\phi,t}}$ in active and reactive ZIP loads, we use the first-order Taylor expansion to linearize it around the ***instantaneous voltage measurements*** $v^{m}_{i,\phi,t-1}$:

$$\sqrt{v_{i,\phi,t}} \approx \bar{v}_{i,\phi,t}$$
$$= v^{m}_{i,\phi,t-1} + \frac{1}{2}(v^{m}_{i,\phi,t-1})^{-1} \odot (v_{i,\phi,t} - v^{m}_{i,\phi,t-1} \odot v^{m}_{i,\phi,t-1})$$

$$p^{ZIP\prime}_{i,\phi,t} \approx p^{ZIP,0}_{i,\phi} \odot (k^{p}_{i,1} v_{i,\phi,t} + k^{p}_{i,2} \bar{v}_{i,\phi,t} + k^{p}_{i,3})$$

$$q^{ZIP\prime}_{i,\phi,t} \approx q^{ZIP,0}_{i,\phi} \odot (k^{q}_{i,1} v_{i,\phi,t} + k^{q}_{i,2} \bar{v}_{i,\phi,t} + k^{q}_{i,3})$$

- Replace $\sqrt{v_{i,\phi,t}}$ by $\bar{v}_{i,\phi,t}$ when calculating ZIP loads

Online and Asynchronous Implementation

Initialize parameters

Receive updates

Primary network (leader controller) solves its problem

Each secondary network ($n \in \mathcal{N}^t$) (follower controller) solves its problem

Each secondary network ($n \notin \mathcal{N}^t$) remain unchanged

Check residuals and update penalty factor

Feedback-based linear approximation

Algorithm 1 Online and Asynchronous Implementations of Distributed VVO-CVR

Initialization: Set $t = 0$ and choose $x(0), z_n(0), n = 1, \ldots, N_S$.
repeat
    $t \leftarrow t + 1$.
    If leader controller receives the newly updated $z_{B,n}$ and λ_n from some follower controller n, then $\mathcal{M}^t \leftarrow \mathcal{M}^{t-1} \cup \{n\}$.
    Let $\tilde{z}^t_{B,n} \leftarrow z^t_{B,n}, \tilde{\lambda}^t_n \leftarrow \lambda^t_n, n \in \mathcal{M}^t$ and $\tilde{z}^t_{B,n} \leftarrow \tilde{z}^{t-1}_{B,n}, \tilde{\lambda}^t_n \leftarrow \tilde{\lambda}^{t-1}_n, n \notin \mathcal{M}^t$.
    if $|\mathcal{M}^t| \geq \tilde{N}_S$ **then**
        Update x^{t+1} by (7) using $\tilde{z}^t_{B,n}$.
        Send $x^{t+1}_{B,n}$ to follower controller $n \in \mathcal{M}^t$.
        Reset $\mathcal{M}^t \leftarrow \emptyset$.
    end if
    for every $n \in \mathcal{N}^t$ **do**
        Update z^{t+1}_n by (8).
        Update λ^{t+1}_n by (9).
        Send $z^{t+1}_{B,n}$ and λ^{t+1}_n to leader controller.
    end for
    for every $n \notin \mathcal{N}^t$ **do**
        Let $z^{t+1}_n \leftarrow z^t_n$ and $\lambda^{t+1}_n \leftarrow \lambda^t_n$.
    end for
    Update ρ^t by (10)–(12).
    Update reactive power output of inverters as per z^{t+1}_n.
    Update the nonlinear terms $\varepsilon^p_{ij,\phi,t}, \varepsilon^q_{ij,\phi,t}$ and $\varepsilon^v_{i,\phi,t}$ by (13)–(15) with measurements feedback from the system.
    Update the estimation of the nonlinear term $\bar{v}_{i,\phi,t}$ in ZIP loads (16)–(18) with measurements feedback from the system.
until t terminates.

Online implementation:

- In each iteration k, the leader and follower controllers use the feedback-based linear approximation method with power and voltage measurement feedback from the system with the last-minute dispatch.

Asynchronous implementation:

- If nth follower controller does not update the variables at iteration k, then the values of λ_n, $x_{B,n}$ and $z_{B,n}$ remain unchanged until the newly updated values come.

Simulation: Setup

A ***real-world distribution feeder*** in Midwest U.S.

- 1 primary network with overhead lines (red) and underground lines (blue).
- 44 secondary networks, a circled capital letter *S*.
- Each secondary network includes a service transformer, a secondary circuit with multiple customers and DERs.
- The time-series multiplier of load demand and solar power with 1-min time resolution.
- The choice of hyper-parameter depends on cross-validation.
- ZIP coefficients of active and reactive loads.

Description	Notion	Value
Initial penalty factor	ρ	0.05
Updating factor	μ	10
Increasing/Decreasing factor	$\tau^{\text{inc}}, \tau^{\text{dec}}$	5,5
Active load ZIP Coefficients	k_1^p, k_2^p, k_3^p	0.96, −1.17,1.21
Reactive load ZIP Coefficients	k_1^q, k_2^q, k_3^q	6.28, −10.16,4.88

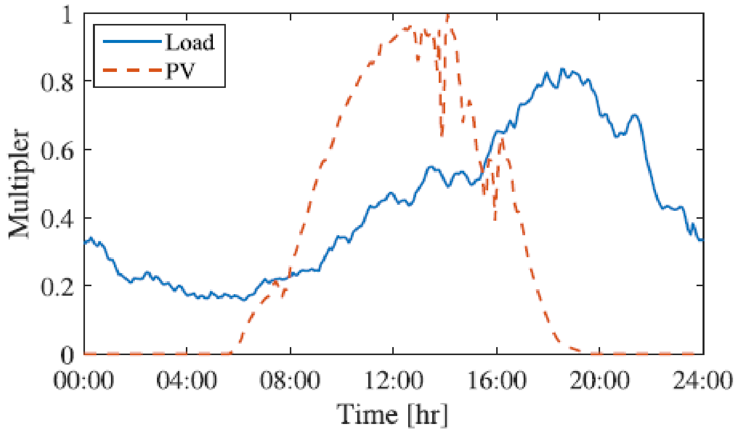

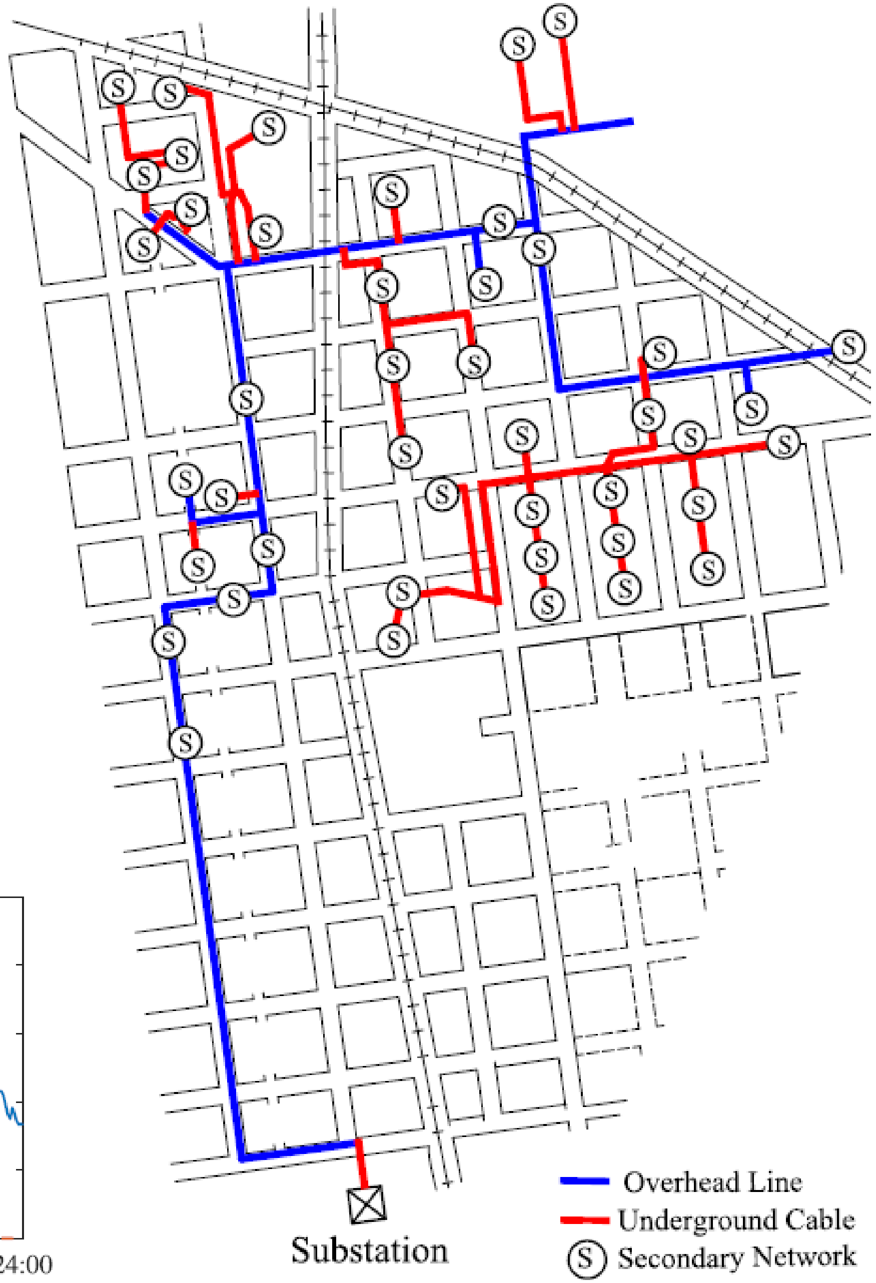

Simulation: Convergence

- The performance for different number of secondary networks (follower controllers) in the asynchronous distributed algorithm is presented.
- The secondary networks are randomly selected in each iteration to ***imitate*** the possible communication failure or delay in the practical cases.

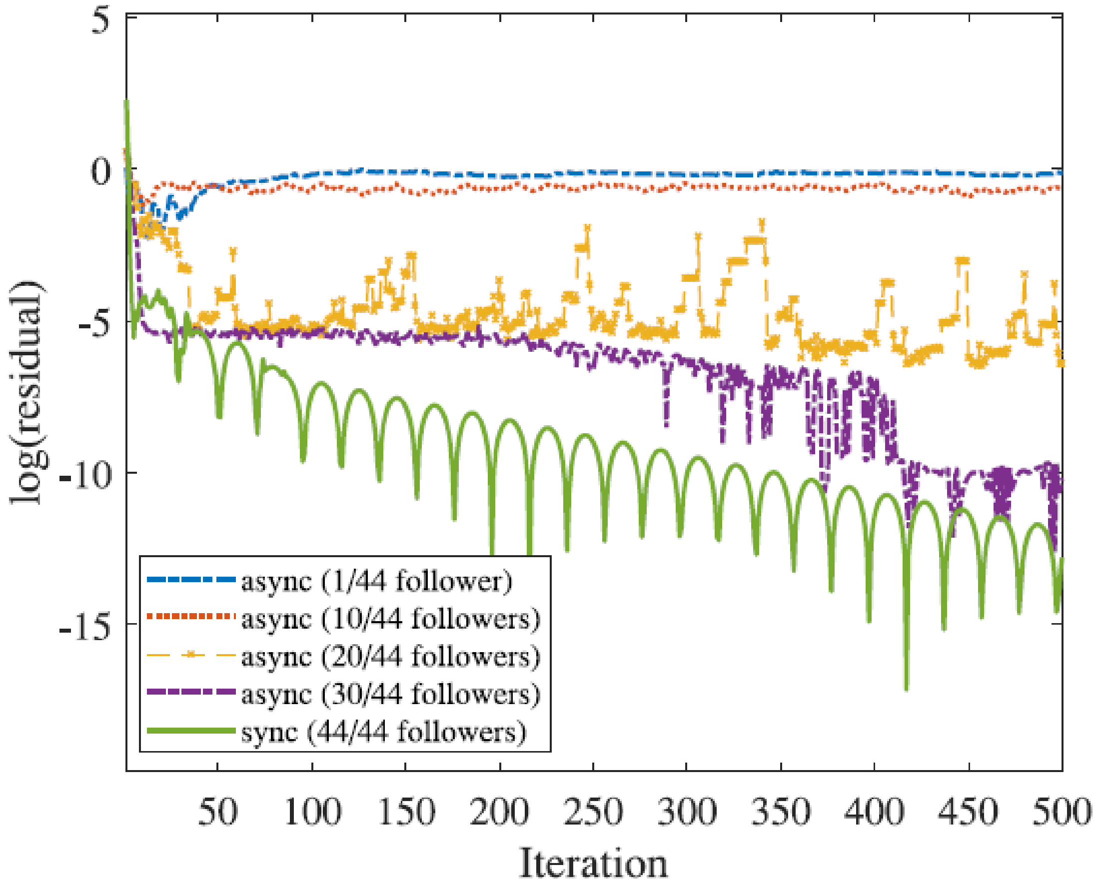

- The log value of primal residual r_n^k is considered as one indicator of the convergence speed:

$$r_n^k = A_n \odot x_{B,n}^k + B_n \odot z_{B,n}^k$$

- No communication failure or delay
- 20 (purple dotted line) or 30 (yellow dotted line) activated secondary networks
- 10 or even fewer activated secondary networks
- ***Trade-off*** between the work stress on communication system and the performance of convergence

We choose ***20 secondary networks*** with the acceptable convergence speed (r_n^k is lower than 10^{-3} around 20 iterations)

Simulation: Convergence

- To show the impacts of the potential failure of the ***primary network (leader controller)***, the convergence speeds of normal communication and communication failure of primary network (leader controller) are compared.
- We assume that the primary network (leader controller) could have communication failure by not updating it own sub-problem and communication during 30th to 50th iteration, then recover the communication at 51st iteration.

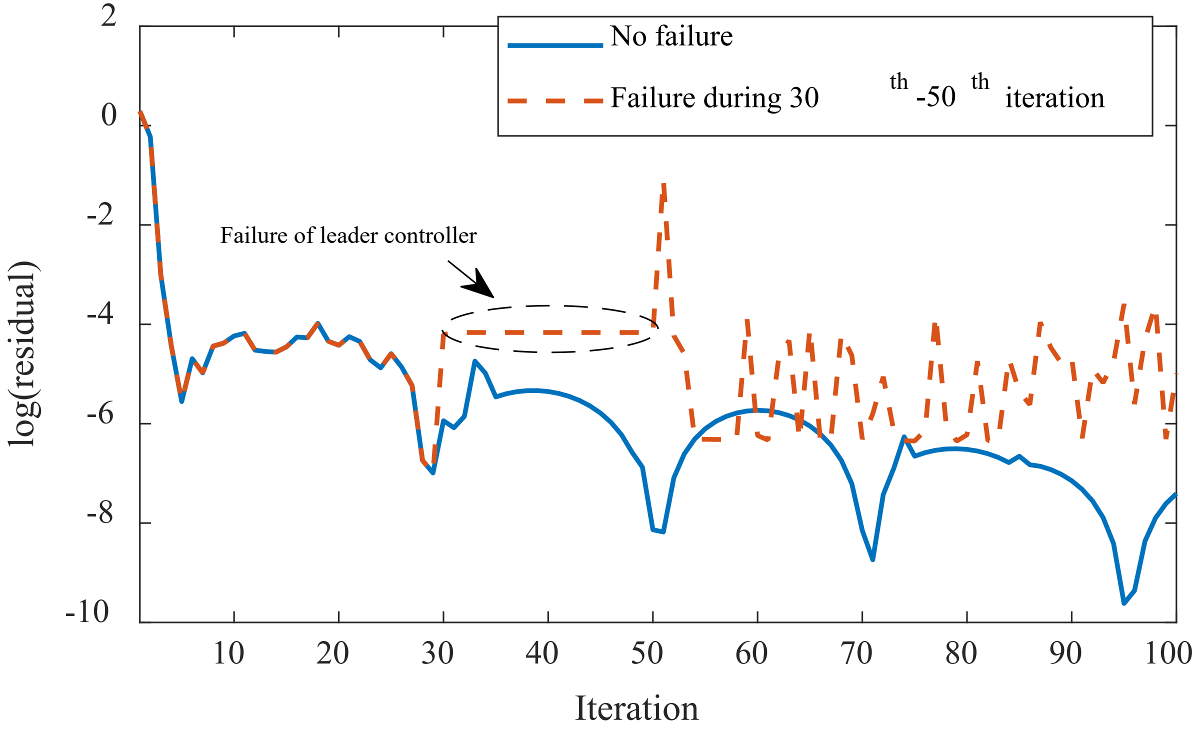

- The overall convergence speed is still acceptable even the primary network fails to update and communicate for 20 iterations.
- Our proposed method is still efficient for ***certain level of communication failure*** of primary network (leader controller).

Simulation: Approximation Errors

- To show the effect of the approximation of the nonlinear part $\sqrt{v_{i,\phi,t}}$, we show the difference between the accurate ZIP load and the approximate ZIP load with a give time series voltage (24 hours with 1-min time resolution).

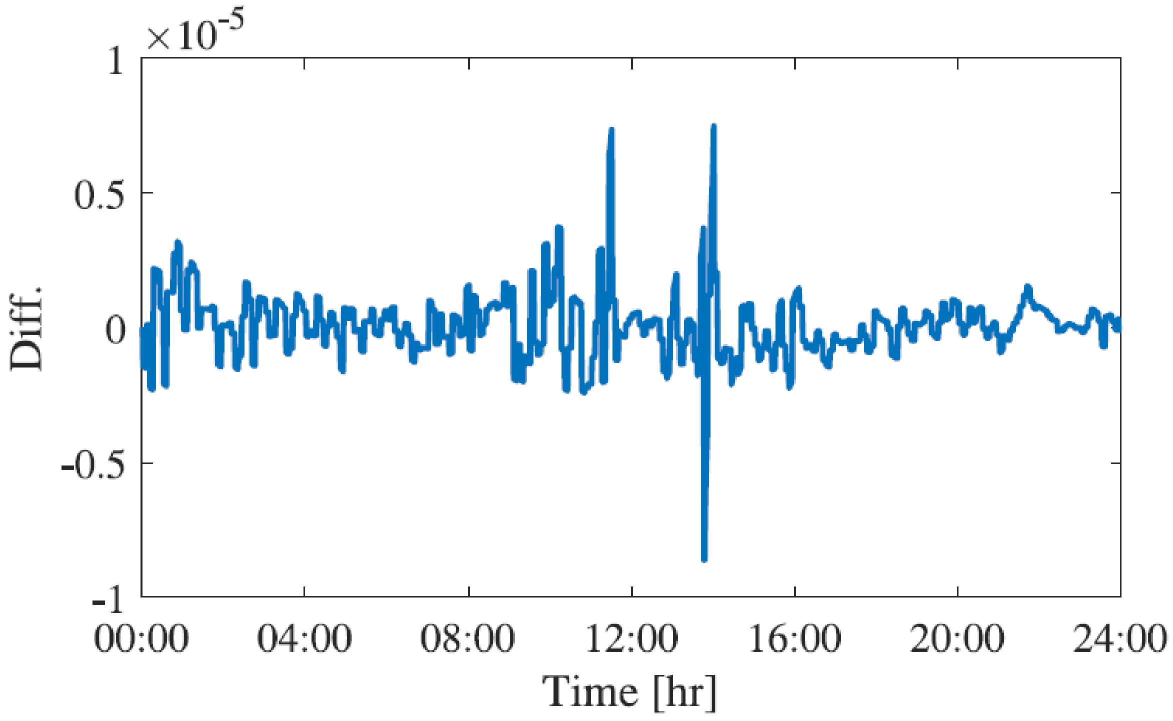

- The ***differences*** between the accurate ZIP load and the approximate ZIP load are ranging from -10^{-5} to 10^{-5}.

$$p_{i,\phi,t}^{ZIP} = p_{i,\phi,t}^{ZIP,0} \odot \left(k_{i,1}^{p} v_{i,\phi,t} + k_{i,2}^{p} \sqrt{v_{i,\phi,t}} + k_{i,3}^{p}\right)$$

$$p_{i,\phi,t}^{ZIP\prime} \approx p_{i,\phi}^{ZIP,0} \odot \left(k_{i,1}^{p} v_{i,\phi,t} + k_{i,2}^{p} \bar{v}_{i,\phi,t} + k_{i,3}^{p}\right)$$

$$\sqrt{v_{i,\phi,t}} \approx \bar{v}_{i,\phi,t}$$

$$= v_{i,\phi,t-1}^{m} + \frac{1}{2}\left(v_{i,\phi,t-1}^{m}\right)^{-1} \odot \left(v_{i,\phi,t} - v_{i,\phi,t-1}^{m} \odot v_{i,\phi,t-1}^{m}\right)$$

Simulation: Grid-Edge Voltage Profile

- We solve the optimal VVO-CVR problem with and without considering the detailed secondary network models.
- Then we input the optimal reactive power dispatch results of smart inverters in the distribution system (OpenDSS) to evaluate the grid-edge voltages.

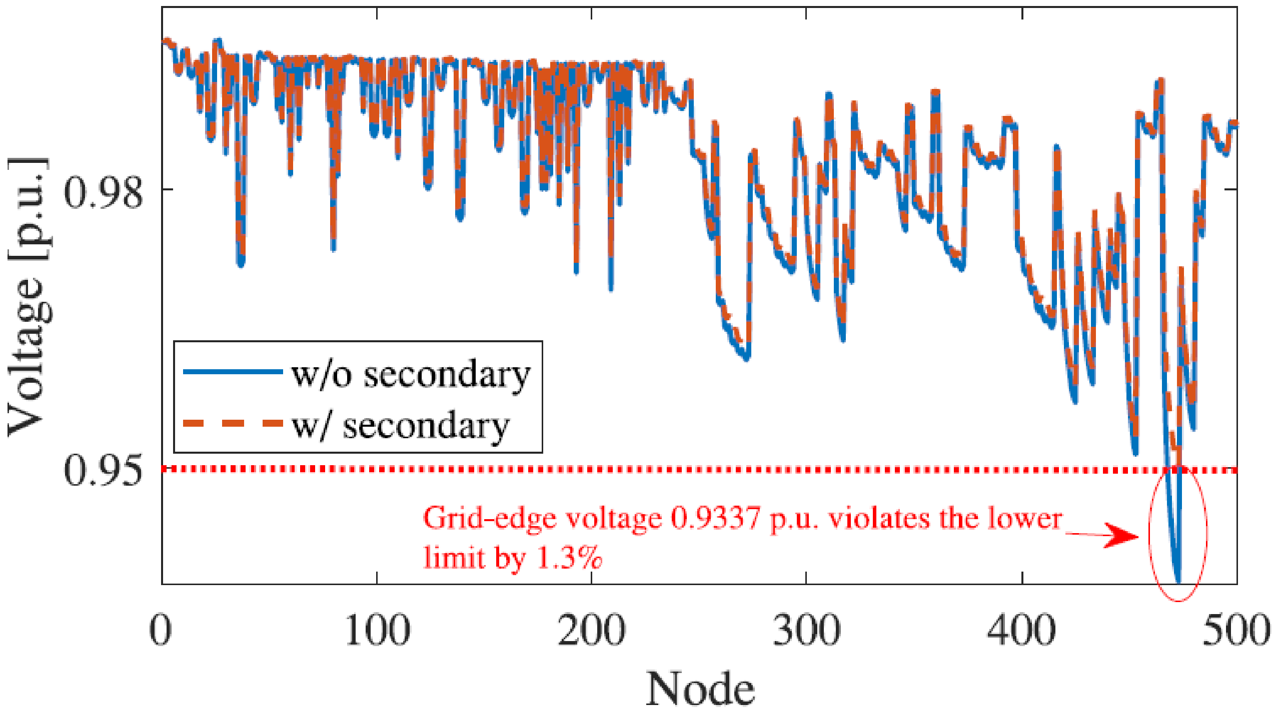

- The ***grid-edge voltage*** can be well regulated if the secondary networks are considered in the VVO-CVR problem.
- If we aggregate secondary networks as nodal injections, the grid-edge voltage within one secondary network is 0.9377 p.u., which violates the voltage lower limit by 1.3%.

Simulation: Reactive Power Dispatch of Smart Inverter

To show the reactive power dispatch behavior of inverters in a clear way, we select two inverters with different locations as examples:

- The inverter 1 (blue) is installed in the end of the secondary network
- The inverter 2 (red) is installed in the middle of the secondary network

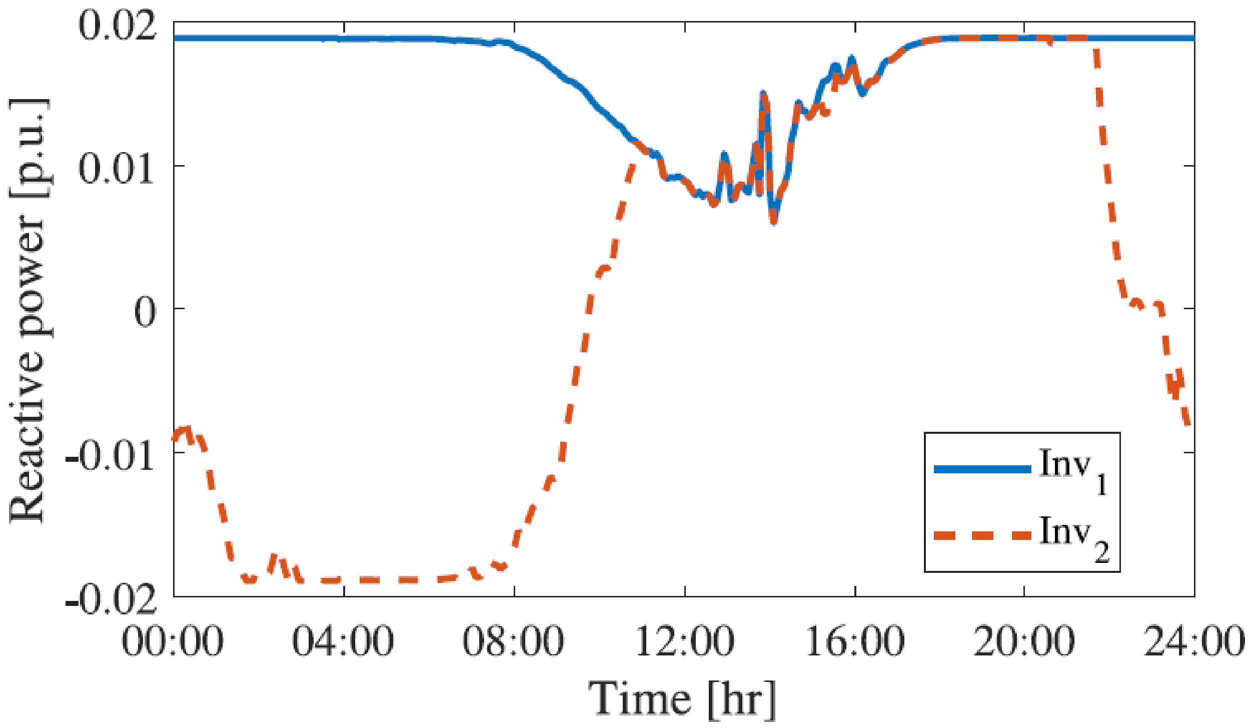

- For inverter 1, the reactive power injections are always required to maintain the voltage above the lower limit.
- For inverter 2, the reactive power injection and absorbing are both required to maintain the voltage within predefined voltage limits.

Simulation: Comparison

We demonstrate the effectiveness of our proposed method by comparing:

- Base case is generated by setting the unity-power factor control mode for all smart inverters where no additional reactive power support is considered.
- Centralized VVO-CVR (CCVR) neglects the nonlinear terms
- ***Distributed asynchronous VVO-CVR (DACVR)***

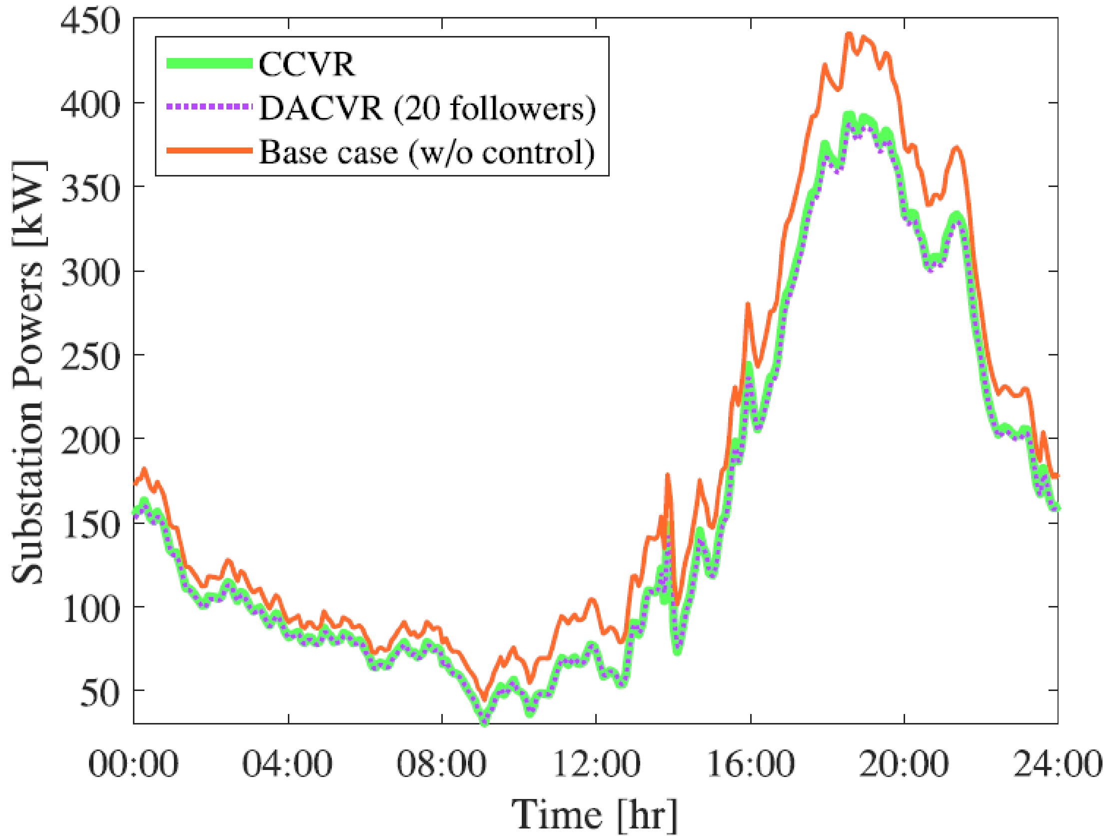

- Compared to base case, the proposed DACVR can effectively reduce the power supply from substation, especially during the peak load period, e.g., 16:00–20:00.
- Compared to CCVR, the proposed DACVR can ***provide a similar control performance***.
- Compared to CCVR, the proposed DACVR ***maintain the data privacy*** of customers.

Simulation: Comparison

The numerical comparisons of total energy consumption over one day and the energy reduction are presented:

- Distributed synchronous VVO-CVR (DSCVR)

	Energy (kWh)	Reduction (%)
Base case (w/o control)	262,167.4	-
CCVR	227,269.9	13.3%
DSCVR	226,339.5	13.6%
DACVR (20 followers)	227,325.1	13.2%

- Because of the neglecting nonlinear terms in power flow model, CCVR cannot obtain the accurate solution.
- DACVR obtains the solution by receiving updates from limited number of secondary networks (follower controllers).
- DSCVR has the online power and voltage feedback measurements from the system to accurately approximate the nonlinear terms of the power flow model and ZIP models.
- DSCVR can receive updates from all the secondary networks (follower controllers).

Simulation: Comparison

- The 1440-minute time-varying voltage profiles of the based case and DACVR are compared.
- Each line represents a phase-wise voltage magnitude of a bus.

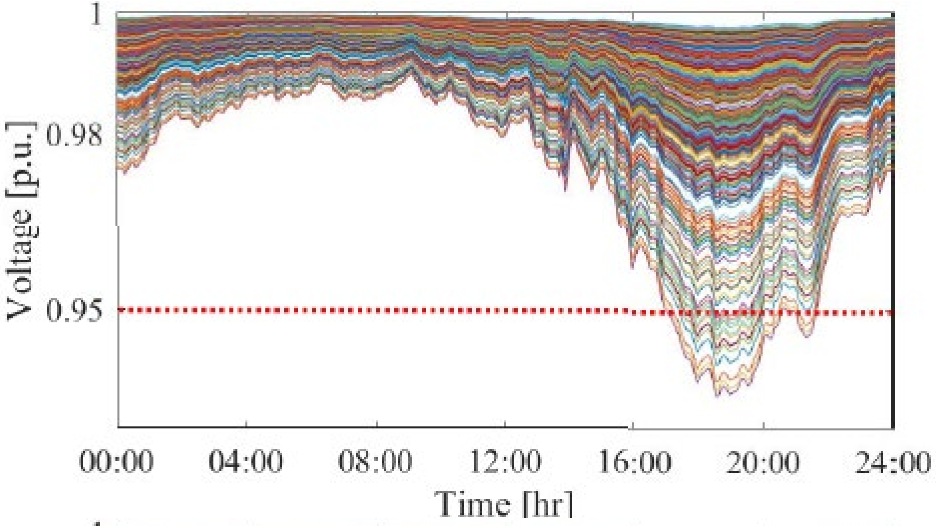

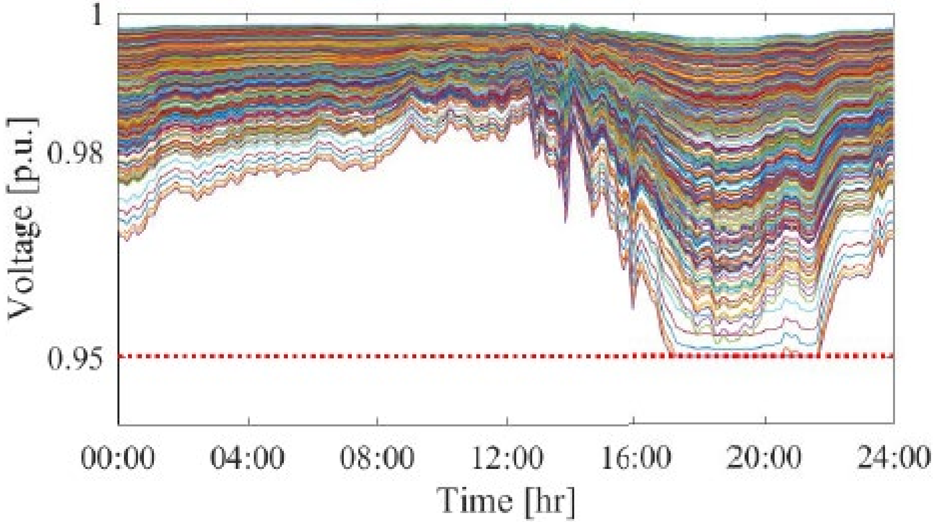

- When there is no reactive power control in the base case, there are voltage violations of the lower voltage limit, during the peak load periods, 16:00-20:00.
- When CVR is implemented with optimal reactive power control, the system ***achieves maximum voltage reduction*** while ***maintains voltage levels with the predefined range***.

Data-based VVC model

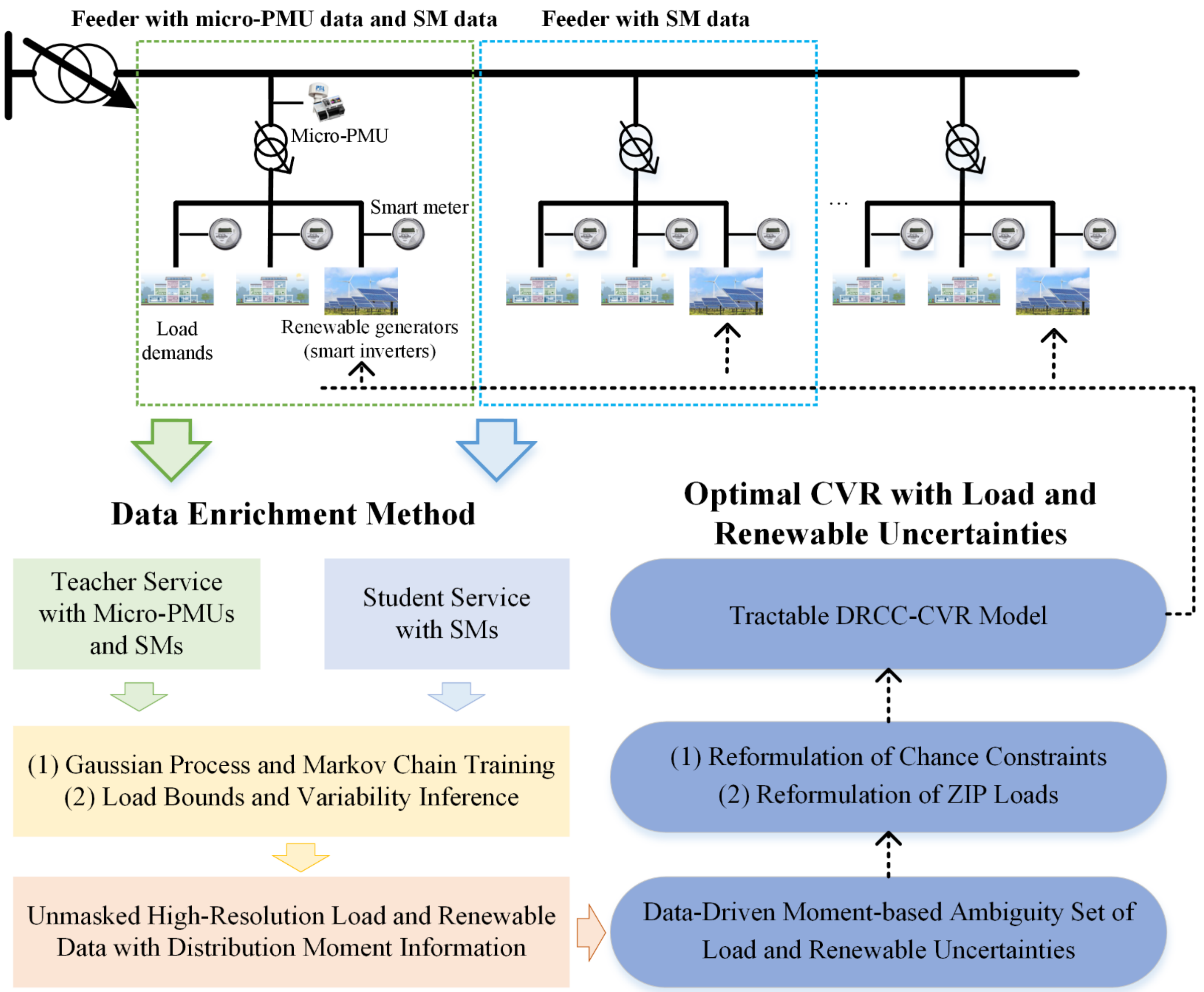

- **Uncertainty of renewable and load**
  - Data-enhancement method
  - Ambiguity set of load and renewable energy uncertainties
- **Distributionally robust chance-constraint model**
  - Distributionally robust chance-constraint optimization
  - Tractable approximation

Multi-agent graph convolutional RL for load restoration

- **Sequential load restoration with changing network topology**
  - During the sequential load restoration, the system topology keeps changing until the maximum restorable load level is achieved.
  - While changing topology needs re-train process in conventional RL-based control method.
- **Integrate system topology information into the training process**
  - Consider the adjacency matrix and nodal feature vector in the Markov Decision Process
  - Extract topology information in topology embedded graph convolutional network
  - Implement multi-head attention, which enable each neighboring agent to exchange coefficients of weights and bias

Scenarios of Different Restoration Path

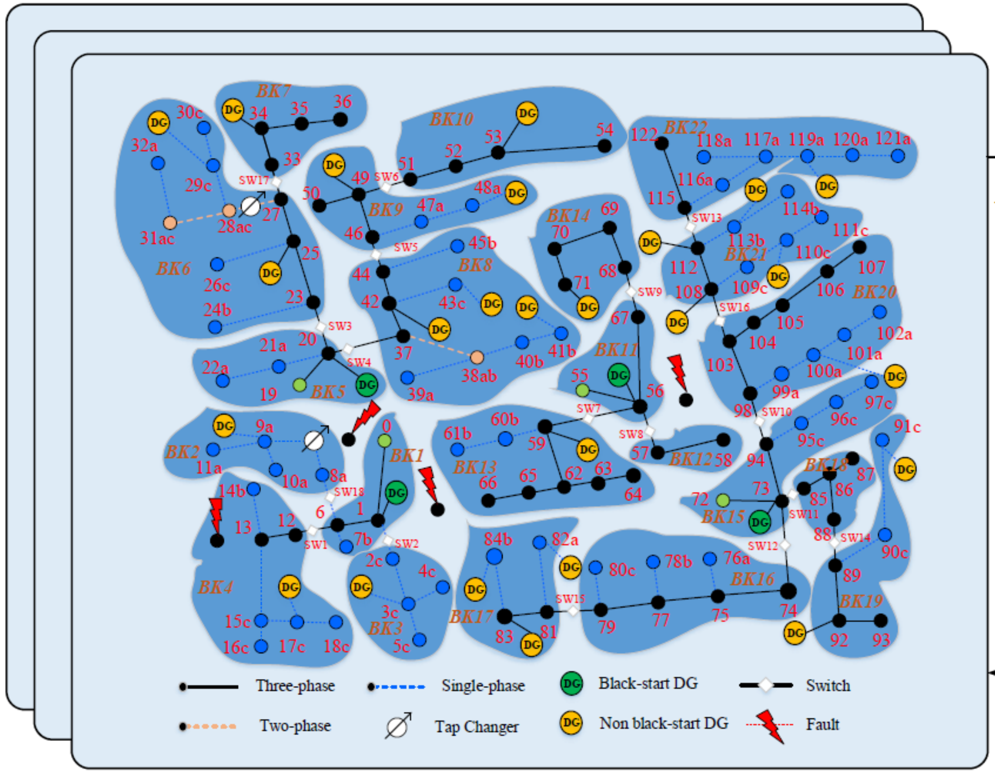

Graph Convolutional Reinforcement Learning

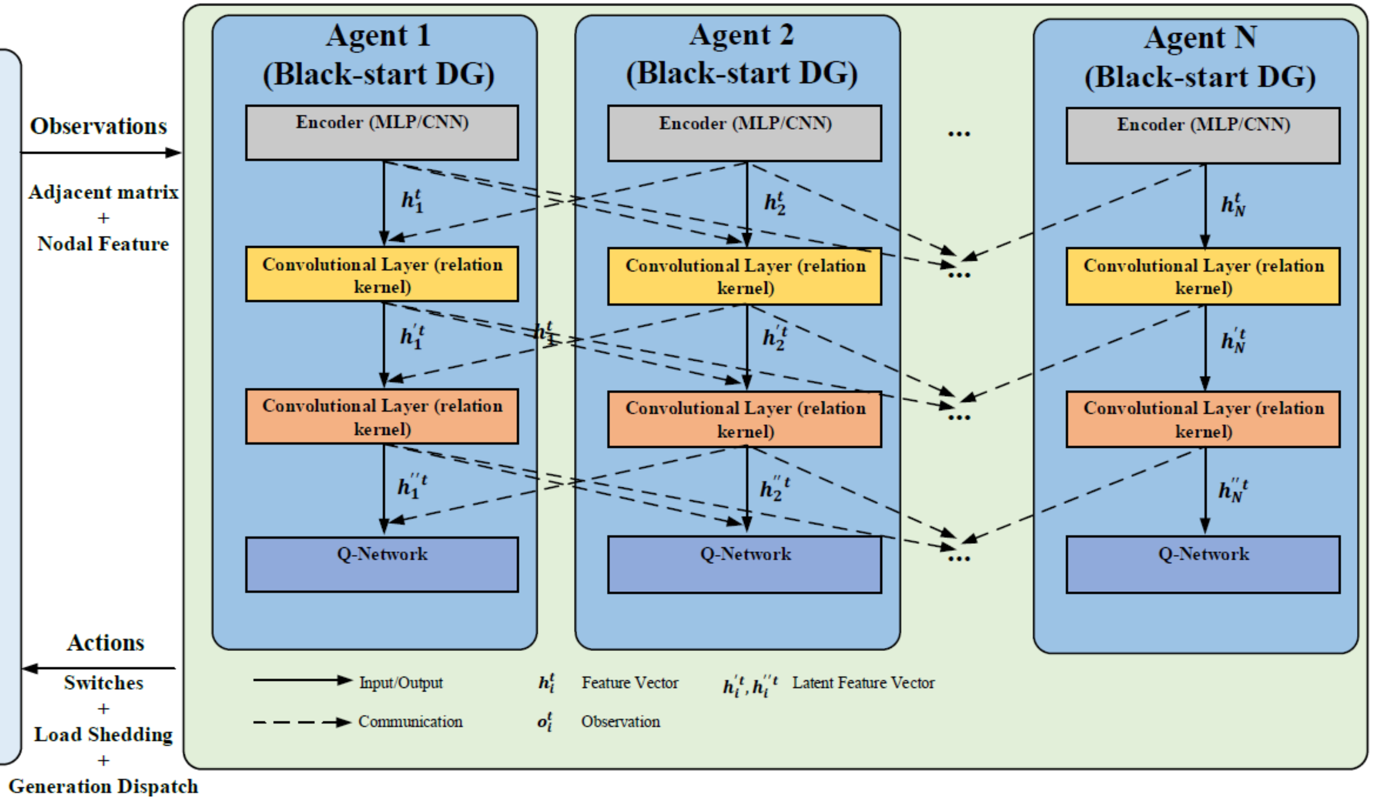

Thank You!
Q & A